



Modelling Rearrangement Process of Martensite Platelets in a Magnetic Shape Memory Alloy Ni₂MnGa Single Crystal under Magnetic Field and (or) Stress Action

J. Y. GAUTHIER,^{1,*} C. LEXCELLENT,² A. HUBERT,¹ J. ABADIE¹ and N. CHAILLET¹

¹Laboratoire d'Automatique de Besançon UMR CNRS 6596
 24 rue Alain Savary, 25000 BESANÇON, France

²Institut FEMTO-ST, Département de Mécanique Appliquée R. Chaléat UMR CNRS 6174
 24 rue de l'Épitaphe, 25000 BESANÇON, France

ABSTRACT: The aim of the paper is the modelling of the rearrangement process between martensite variants in order to use Magnetic Shape Memory alloys (MSMs) as actuators. In the framework of the thermodynamic of irreversible processes, an efficient choice of the internal variables in order to take into account the magnetic and the mechanical actions and a free energy function are stated. The behaviour is chosen as magnetically reversible and mechanically irreversible. An equivalence between magnetic field action H and uniaxial stress action σ for the initiation of the rearrangement is established. Finally, model predictions are compared with experimental measurements.

Key Words: Magnetic shape memory alloys, Reorientation process, Single crystal, Actuator, Modelling.

INTRODUCTION

Magnetic Shape Memory alloys (MSMs) are attractive materials because they can be controlled not only by stress and temperature actions as the classical Shape Memory Alloys (SMAs) but also by a magnetic field. They also present a response time 100 times shorter than classical SMAs while the two types of alloys present equivalent performances in term of deformation amplitude (about 6 % for a complete phase transformation for SMAs or reorientation process for MSMs). In the present paper, a particular attention is paid to the modelling of the Ni₂MnGa single crystal thermo-magneto-mechanical behaviour.

Thanks to classical SMAs, the mechanical contribution is well understood while the magnetic one is nowadays more delicate to integrate in a model. Thermodynamic of Irreversible Processes (T.I.P.) is used and efficient internal variables are chosen in

order to build a thermodynamical potential. With an average method of micromechanics (Mori and Tanaka, 1973), a macroscopic Gibbs free energy function is derived for the (n+1) phases mixture i.e. one austenite phase and n martensite variants in the single crystal.

The first part of this paper will propose an expression for the Gibbs free energy. A special attention is devoted to the rearrangement process between two variants of martensite M_1 and M_2 under the stress action and (or) the magnetic field. In a second part, this energy expression will be completed with the Clausius-Duhem inequality (corresponding to an irreversible behaviour), the kinetic equation (modelling of the hysteretic internal loop) and the heat equation. Then, a complete magneto-thermo-mechanical model is obtained. In the final part, we will compare this model with experimental measurements.

At the end of the paper, a glossary defines all variables.

INTERNAL VARIABLES MODEL RELATED TO THE MSM SINGLE CRYSTAL BEHAVIOUR

The MSM sample Gibbs free energy G expression can be split into four parts: the chemical contribution G_{chem} (generally associated to the latent heat of the phase transformation), the mechanical one G_{mech} , the magnetic one G_{mag} and the thermal one G_{therm} (associated to the heat capacity).

$$G(\underline{\Sigma}, T, \vec{H}, z_o, z_1, \dots, z_n, \alpha, \theta) = G_{chem}(T, z_o) + G_{mech}(\underline{\Sigma}, z_o, z_1, \dots, z_n) + G_{mag}(\vec{H}, z_o, \dots, z_n, \alpha, \theta) + G_{therm}(T) \quad (1)$$

where the state variables are:

- $\underline{\Sigma}$: applied stress tensor,

*Author to whom correspondence should be addressed.
 E-mail: jean-yves.gauthier@ens2m.fr

- \vec{H} : magnetic field,
- T : temperature.

The internal variables are:

- z_o : austenite volume fraction,
- z_k : volume fraction of martensite variant k ($k \in \{1; n\}$), i.e. the martensite presents n different variants. Let $\sum_{k=1}^n z_k = (1 - z_o)$ be the global fraction of martensite,
- α and $(1 - \alpha)$ the proportions of the Weiss domains inside a variant representing the Representative Elementary Volume (REV) (figure 1) (Hirsinger and Lexcellent, 2002),
- θ the rotation angle of the magnetization vector associated to the two Weiss domains of variant M_2 . Indeed, under the magnetic field \vec{H} , this magnetization rotates in order to become parallel to the magnetic field. As the field \vec{H} is parallel to \vec{x} , there is no rotation of Weiss domains of variant M_1 (Creton, 2004; Hirsinger et al., 2004).

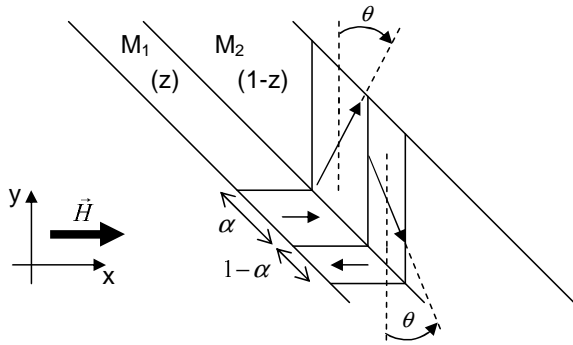


Figure 1. Representative Elementary Volume (REV) when the MSM sample is only composed of two martensite variants M_1 and M_2 ($z = z_1$ and $1 - z = z_2$) (Hirsinger and Lexcellent, 2002).

The four terms of the free energy expression can be examined as follow:

Chemical Energy

As all chemical energies of different martensite variants are the same:

$$G_{chem} = z_o(u_o^A - Ts_o^A) + (1 - z_o)(u_o^M - Ts_o^M) \quad (2)$$

This can also be expressed as:

$$G_{chem} = (u_o^M - Ts_o^M) - z_o\pi_o^f(T) \quad (3)$$

with $\pi_o^f(T) = \Delta u - T\Delta s$, $\Delta u = u_o^A - u_o^M$ and $\Delta s = s_o^A - s_o^M$.

$\pi_o^f(T)$ represents the thermodynamical force associated with the thermal induced phase transformation.

Thermal Energy

The expression of the thermal energy is chosen as:

$$G_{therm} = C_p \left[(T - T_o) - T \cdot \log \left(\frac{T}{T_o} \right) \right] \quad (4)$$

This expression guarantees that the specific heat C_p agrees with:

$$C_p = -T \frac{d^2 G_{therm}}{dT^2} \quad (5)$$

Mechanical Energy

The expression of the mechanical energy is chosen as:

$$\rho G_{mech}(\underline{\Sigma}, T, z_o, z_1, \dots, z_n) = -\underline{\Sigma} : \left(\sum_{k=0}^n z_k \underline{E}_k^{tr} \right) - \frac{1}{2} \underline{\Sigma} : \underline{S} : \underline{\Sigma} + \phi_{it}(z_o, \dots, z_n) \quad (6)$$

with:

$$\phi_{it} = Az_o(1 - z_o) + \frac{1}{2} \sum_{k=1}^n \sum_{\substack{\ell=1 \\ \ell \neq k}}^n K_{k\ell} z_k z_\ell \quad (7)$$

and

$$\sum_{k=0}^n z_k = 1 \quad (8)$$

when \underline{S} is the elastic compliance tensor (chosen independent of the phase state).

The first term of the expression of ϕ_{it} , including the material parameter A , represents the austenite-global martensite interaction. The second term, including the material parameters $K_{k\ell}$, represents the interaction between martensite variants ($K_{k\ell}$ is associated with the interaction between variants M_k and M_ℓ).

As it was previously underlined (Patoor et al., 1998; Sun and Hwang, 1993; Lexcellent et al., 1996), the G_{mech} expression depends on the choice of ϕ_{it} permitting the differentiation between some "micro-macro" models. In Buisson et al. (1991), the global behaviour associated to the interfaces displacement between martensite variants is analyzed.

In a classical way, the total strain tensor $\underline{\varepsilon}$ and the thermodynamical force π_k^f associated with the progress of the M_k variant can be defined as:

$$\underline{\varepsilon} = -\frac{\partial \rho G}{\partial \underline{\Sigma}} \quad , \quad \pi_k^f = -\frac{\partial \rho G}{\partial z_k} \quad (9)$$

Then,

$$\underline{\varepsilon} = \underline{S} : \underline{\Sigma} + \sum_{k=0}^n z_k \underline{E}_k^{tr} \quad (10)$$

The left member of equation (10) corresponds to the classical elastic strain tensor. The right member corresponds to the phase transformation strain (between austenite and one variant of martensite) or reorientation of martensite platelets.

$$\pi_o^f = \underline{\Sigma} : \underline{E}_o^{tr} - A(1 - 2z_o) \quad (\text{phase transformation}) \quad (11)$$

$$\pi_k^f = \underline{\Sigma} : \underline{E}_k^{tr} - K_{k\ell} z_\ell \quad (k \in \{1; n\}) \quad (\text{reorientation}) \quad (12)$$

The Clausius-Duhem inequality can be written, then the dissipation increment is:

$$dD = \sum_{k=0}^n \pi_k^f dz_k \geq 0 \quad (13)$$

Crystallography of the Ni₂MnGa

The parent austenitic phase exhibits a cubic structure called $L2_1$ (the lattice parameter a_o is chosen around 5.82 Å and is considered independent of the alloy composition and temperature). Under cooling or stress action, this alloy can generate three different martensitic phases:

- the modulated five-layered martensite (Quadratic 5M) with an induced strain in the order of 6 %,
- the modulated seven layered martensite structure (Monoclinic 7M) with 10% of induced strain,
- the non modulated quadratic phase (NMT) 16 to 20%.

The present paper is devoted to the most common Ni₂MnGa martensite e.g. the 5M. This alloy was used and a 2.5% strain up to 500 Hz was performed (Henry et al., 2002; Marioni et al., 2003). The Ni₂MnGa MSM element applied as a sensor is investigated by Mullner et al. (2003) and Suorsa et al. (2004).

\underline{U}_i describes the homogeneous deformation that takes the lattice of the austenite to that of martensite and is called the "Bain matrix" or the "Phase Transformation Matrix". The austenite → martensite 5M Phase Transformation corresponds to a cubic to tetragonal phase transformation.

The transformation matrix is given by:

$$\underline{U}_1 = \begin{pmatrix} \beta_c & 0 & 0 \\ 0 & \beta_a & 0 \\ 0 & 0 & \beta_a \end{pmatrix} \quad (14)$$

where $\beta_a = \frac{a}{a_o}$ and $\beta_c = \frac{c}{a_o}$ with respect to the lattice cubic austenite cell (figure 2).

The two matrix corresponding to the others variants are:

$$\underline{U}_2 = \begin{pmatrix} \beta_a & 0 & 0 \\ 0 & \beta_c & 0 \\ 0 & 0 & \beta_a \end{pmatrix} \quad \text{and} \quad \underline{U}_3 = \begin{pmatrix} \beta_a & 0 & 0 \\ 0 & \beta_a & 0 \\ 0 & 0 & \beta_c \end{pmatrix} \quad (15)$$

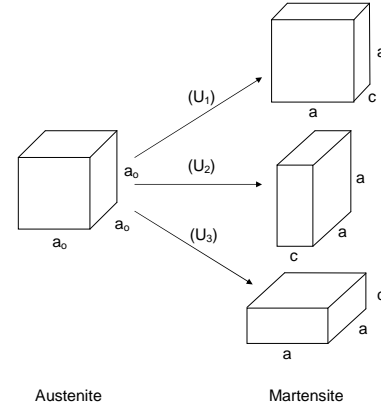


Figure 2. The three variants of martensite in a cubic to tetragonal transformation.

Following the Crystallographic Theory of Martensite (C.T.M. theory) (Ball and James, 1987; Ball and James, 1992), an exact interface between the parent phase A and a single variant of martensite exists if and only if \underline{U}_i presents an eigenvalue λ_2 equal to 1 with $\lambda_1 \geq \lambda_2 \geq \lambda_3$.

This condition constitutes a theorem of Ball and James and the condition is fulfilled, for instance, for same cubic → monoclinic phase transformation on CuAlZn, CuAlBe alloys which presents one variant of martensite-austenite interface (Hane, 1999).

But, this is not the case for Ni₂MnGa. As an example, for Ni_{51.3}Mn_{24.0}Ga_{24.7}, $\lambda_1 = \lambda_2 = \beta_a = 1.013$ and $\lambda_3 = \beta_c = 0.952$ (James and Zhang, 2005). It results that there is an interface between austenite and a twin of martensites variants (M_i, M_j). At first, one examines the compatibility equation between the variants of martensite themselves which is called the "twinning equation":

$$\underline{Q}\underline{U}_i - \underline{U}_j = \vec{a} \otimes \vec{n} \quad (16)$$

where \underline{Q} is a rotation matrix, \vec{n} the unit vector normal to the interface and \vec{a} the "shear vector" (see figure 3).

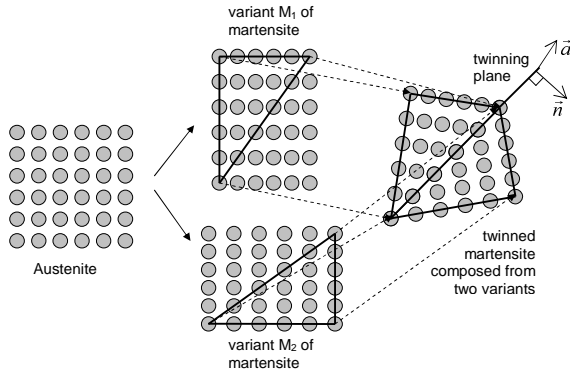


Figure 3. A schematic 2-dimensional situation: a "cubic" grid (left), its martensitic transformation (middle) and twins created by matching two slightly rotated triangles of both martensitic variants (right)(Roubíček, 2004).

The solutions for the cubic to tetragonal transformation are:

$$\vec{a} = \frac{\sqrt{2}(\beta_a^2 - \beta_c^2)}{(\beta_c^2 + \beta_a^2)} \begin{pmatrix} \beta_c \\ -\beta_a \\ 0 \end{pmatrix} \quad \vec{n} = \frac{1}{\sqrt{2}} \begin{pmatrix} 1 \\ 1 \\ 0 \end{pmatrix}$$

or

$$\vec{a} = \frac{\sqrt{2}(\beta_a^2 - \beta_c^2)}{(\beta_c^2 + \beta_a^2)} \begin{pmatrix} \beta_c \\ \beta_a \\ 0 \end{pmatrix} \quad \vec{n} = \frac{1}{\sqrt{2}} \begin{pmatrix} 1 \\ -1 \\ 0 \end{pmatrix} \quad (17)$$

For the twinning elements, the twinning shear s' relative to the lattice or twin plane is given, in the general case, by Bhattacharya (2003):

$$s' = |\vec{a}| |U_j^{-1} \vec{n}| \quad (18)$$

and, in the special case of tetragonal Ni_2MnGa , by:

$$s' = \left| \frac{\beta_a}{\beta_c} - \frac{\beta_c}{\beta_a} \right| = \left(\frac{a}{c} - \frac{c}{a} \right) \quad (19)$$

Each pair of variants (U_i, U_j) can form a twin and all the twins are compound with the $(110)_{cubic}$ twin plane.

From now, the martensite variants reorientation process is considered under stress action in one direction and magnetic field action perpendicularly to this direction (see figure 4).

Let z_1 be the volume fraction of variant M_1 ($z_1 = z$) and z_2 the volume fraction of variant M_2 ($z_2 = 1 - z$).

Let us consider that the material is initially only made up of the variant M_1 ($z_0 = 0, z_1 = 1, z_2 = 0$) and is transformed under mechanical loading in the variant M_2 . The compatibility conditions between M_1 and M_2 are verified.

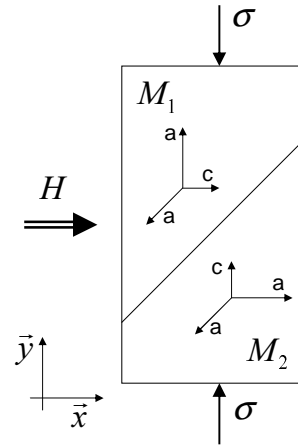


Figure 4. The MSM sample is subject to a compressive stress in the \vec{y} direction and to a magnetic field in the \vec{x} direction.

The tensor stress can be written as:

$$\underline{\Sigma} = \begin{pmatrix} 0 & 0 & 0 \\ 0 & +\sigma & 0 \\ 0 & 0 & 0 \end{pmatrix} \quad (20)$$

with $\sigma > 0$ for tension and $\sigma < 0$ for compression.

If we note \underline{E}_i , the transformation gradient of austenite A into martensite M_i is:

$$d\vec{x}_o(A) \xrightarrow{\underline{E}_i} d\vec{x}(M_i) \quad (21)$$

the Green-Lagrange deformation tensor \underline{E}_i^{tr} is then defined by:

$$\underline{E}_i^{tr} = \frac{1}{2} ({}^t \underline{E}_i \underline{E}_i - \underline{1}) \quad \text{with } {}^t \underline{E}_i \underline{E}_i = \underline{U}_i^2 \quad (22)$$

$$\underline{E}_i^{tr} = \frac{1}{2} (\underline{U}_i^2 - \underline{1}) \quad (23)$$

In this simple case, equation (6) of the mechanical free energy is reduced to:

$$\rho G_{mech}(\sigma, T, z) = -\sigma \left(\left(\frac{\beta_a^2 - \beta_c^2}{2} \right) z + \frac{\beta_c^2 - 1}{2} \right) - \frac{1}{2} \frac{\sigma^2}{E} + K_{12} z (1 - z) \quad (24)$$

with $K_{ij} = K_{ji}$ and $\frac{\beta_a^2 - \beta_c^2}{2} = \gamma$ ($= 0.06$ with the precedent data).

The term $\frac{\beta_c^2 - 1}{2}$ will be neglected and the state for $z = 0$ will be considered as not strained.

Thanks to equation 24, the total macroscopic deformation is obtained:

$$\varepsilon_{yy} = \varepsilon = -\rho \frac{\partial G_{mech}}{\partial \sigma} = \frac{\sigma}{E} + \gamma z = \varepsilon^e + \varepsilon^{dtw} \quad (25)$$

where "dtw" means "detwinning".

Let π^f be the thermodynamic force associated to the reorientation of variant M_2 in variant M_1 :

$$\pi^f = -\frac{\partial \rho G_{mech}}{\partial z} = \sigma\gamma - K_{12}(1-2z) \quad (26)$$

In the case of $M_2 \rightarrow M_1$, the dissipation increment dD can be expressed as:

$$dD = \pi^f dz \geq 0 \quad (27)$$

Magnetic Energy

As established by Landau and Lifshitz (1984) and Sommerfeld (1964), the incremental magnetic energy density can be expressed as:

$$du_{mag} = \vec{H} \cdot d\vec{B} \quad (28)$$

with \vec{H} the magnetic field and \vec{B} the magnetic flux density.

If this energy is present into a material with \vec{M} the magnetization of the medium and μ_0 the permeability of the vacuum, then, as $\vec{B} = \mu_0(\vec{H} + \vec{M})$, the following expression can be obtained:

$$\begin{aligned} du_{mag} &= \vec{H} \cdot d(\mu_0(\vec{H} + \vec{M})) \\ &= \mu_0 \vec{H} \cdot d\vec{H} + \mu_0 \vec{H} \cdot d\vec{M} \end{aligned} \quad (29)$$

As noticed by Sommerfeld, the first term $\mu_0 \vec{H} \cdot d\vec{H}$ can be neglected because it is present even in the absence of magnetization of the material and will disappear in the final energy conversion. For this reason, in the future computation, the following equality will be used:

$$du_{mag} = \mu_0 \vec{H} \cdot d\vec{M} \quad (30)$$

Concerning the magnetic field, it is more useful to manipulate the magnetic co-energy instead of magnetic energy when the control through a current flowing in an external coil is done. This magnetic co-energy u_{mag}^* is deduced by the following Legendre transformation:

$$u_{mag}^* = u_{mag} - \mu_0 \vec{M} \cdot \vec{H} \quad (31)$$

$$du_{mag}^* = du_{mag} - \mu_0 \vec{M} \cdot d\vec{H} - \mu_0 \vec{H} \cdot d\vec{M} \quad (32)$$

$$= -\mu_0 \vec{M} \cdot d\vec{H} \quad (33)$$

Therefore, the magnetic contribution added to the Gibbs free energy is:

$$\rho G_{mag}(\vec{H}) = -\int_0^{\vec{H}} \mu_0 \vec{M} \cdot d\vec{H} \quad (34)$$

In the case described by the figure 1 (Hirsinger and LExcellent, 2002), magnetization is expressed as:

$$\begin{aligned} \vec{M} &= M_S [(2\alpha - 1)z + \sin \theta(1 - z)] \vec{x} + \\ &M_S(2\alpha - 1)(1 - z) \cos \theta \vec{y} \end{aligned} \quad (35)$$

In our modelling, the magnetic field \vec{H} and the magnetization \vec{M} are considered in the \vec{x} direction (the magnitudes are respectively noted H and M)(see figure 4).

Moreover, the experimental observation of the curve (H, M) for different volume fractions of martensite, given in figure 5, shows that: when $z = 1$, the evolution of M is a linear function of H with a slope χ_t ; when $z = 0$, M is a linear function of H with a slope χ_a . Therefore, magnetization contribution can be expressed as:

$$M = M_x = \chi_a H \cdot z + \chi_t H \cdot (1 - z) \quad (36)$$

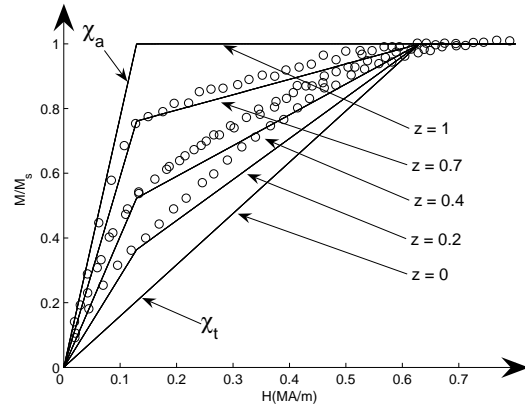


Figure 5. Magnetization curves for different volume fractions of martensite variant 1: model (solid lines) and experiments (o) (experiments are taken from Likhachev et al. (2004)).

Using both expressions of M_x (equations (35) and (36)), the following relations between α and H on the one hand and between θ and H on the other hand.

$$0 \leq \alpha = \frac{\chi_a H}{2M_S} + \frac{1}{2} \leq 1 \quad (37)$$

$$0 \leq \theta = \arcsin\left(\frac{\chi_t H}{M_S}\right) \leq \frac{\pi}{2} \quad (38)$$

For an unidirectional problem, the combination of equations (34) and (35) gives:

$$\begin{aligned} \rho G_{mag} &= \\ &= -\mu_0 M_S \int_0^H ((2\alpha - 1)z + \sin \theta(1 - z)) dh \end{aligned} \quad (39)$$

As z and H are independent variables:

$$\rho G_{mag} = -\mu_o M_S \left(z \int_0^H (2\alpha - 1) dh + (1 - z) \int_0^H \sin \theta dh \right) \quad (40)$$

For the integration, the H domain is split in three cases.

1) First case:

$$H < \frac{M_S}{\chi_a} \text{ e.g. } 0 < \alpha < 1, 0 < \theta < \frac{\pi}{2}$$

$$\Rightarrow \begin{cases} \int_0^H (2\alpha - 1) dh = \int_0^H \frac{\chi_a h}{M_S} dh = \frac{\chi_a H^2}{2M_S} \\ \int_0^H \sin(\theta) dh = \int_0^H \frac{\chi_t h}{M_S} dh = \frac{\chi_t H^2}{2M_S} \end{cases} \quad (41)$$

2) Second case:

$$\frac{M_S}{\chi_a} < H < \frac{M_S}{\chi_t} \text{ e.g. } \alpha = 1, 0 < \theta < \frac{\pi}{2}$$

$$\Rightarrow \begin{cases} \int_0^H (2\alpha - 1) dh = \int_0^{\frac{M_S}{\chi_a}} (2\alpha - 1) dh \\ + \int_{\frac{M_S}{\chi_a}}^H (2\alpha - 1) dh = H - \frac{M_S}{2\chi_a} \\ \int_0^H \sin(\theta) dh = \frac{\chi_t H^2}{2M_S} \end{cases} \quad (42)$$

3) Third case:

$$H > \frac{M_S}{\chi_t} \text{ e.g. } \alpha = 1, \theta = \frac{\pi}{2}$$

$$\Rightarrow \begin{cases} \int_0^H (2\alpha - 1) dh = H - \frac{M_S}{2\chi_a} \\ \int_0^H \sin(\theta) dh = \int_0^{\frac{M_S}{\chi_t}} \sin(\theta) dh \\ + \int_{\frac{M_S}{\chi_t}}^H \sin(\theta) dh = H - \frac{M_S}{2\chi_t} \end{cases} \quad (43)$$

A synthesis of the three previous cases gives:

$$\begin{cases} \int_0^H (2\alpha - 1) dh = (2\alpha - 1)H - \frac{M_S}{2\chi_a} (2\alpha - 1)^2 \\ \int_0^H \sin(\theta) dh = \sin(\theta)H - \frac{M_S}{2\chi_t} (\sin(\theta))^2 \end{cases} \quad (44)$$

Lastly, the expression of the magnetic contribution

of the Gibbs free energy function becomes:

$$\rho G_{mag}(H, z, \alpha, \theta) = -\mu_o M_S \left[z \left((2\alpha - 1)H - \frac{M_S}{2\chi_a} (2\alpha - 1)^2 \right) + (1 - z) \left(\sin(\theta)H - \frac{M_S}{2\chi_t} (\sin(\theta))^2 \right) \right] \quad (45)$$

Gibbs Free Energy Expression for Reorientation Process of Martensite Variants

According to the previous calculations, the free energy expression can finally be reached:

$$\rho G(\sigma, H, T, z, \alpha, \theta) = C_p \left[(T - T_o) - T \cdot \log \frac{T}{T_o} \right] - \sigma \gamma z - \frac{\sigma^2}{2E} + K_{12} z (1 - z) - \mu_o M_S \left(z \left((2\alpha - 1)H - \frac{M_S}{2\chi_a} (2\alpha - 1)^2 \right) + (1 - z) \left(\sin(\theta)H - \frac{M_S}{2\chi_t} (\sin(\theta))^2 \right) \right) \quad (46)$$

This paper deals with rearrangement of martensite platelets and not phase transformation explaining why the "chemical contribution" is not considered. However, the magneto-mechanical expression for the rearrangement between two variants of martensite under magnetic field and (or) stress action is rather complicated.

To determine G , the coupling between mechanic and magnetism is not caused by the choice of a magneto-mechanic $G_{mech,mag}$ expression, but by the choice of the internal variables (z in the considered paper).

GIBBS FREE ENERGY MODEL HANDLING

Calculations of the Different Thermodynamical Forces

In a classical way the total deformation and the magnetization M can be written from (25) and (35) respectively as:

$$\varepsilon = -\frac{\partial(\rho G)}{\partial \sigma} = \frac{\sigma}{E} + \gamma z = \varepsilon^e + \varepsilon^{dtw} \quad (47)$$

$$\mu_o M = -\frac{\partial(\rho G)}{\partial H} \quad (48)$$

$$= \mu_o M_S ((2\alpha - 1)z + \sin \theta (1 - z)) \quad (49)$$

The thermodynamical force associated with the progression of the Weiss domain width α and rotation angle of the magnetization θ are:

$$\frac{\partial(\rho G)}{\partial \alpha} = -2\mu_o M_S z \left(H - \frac{M_S}{\chi_a} (2\alpha - 1) \right) = 0 \quad (50)$$

$$\frac{\partial(\rho G)}{\partial \theta} = -\mu_o M_S (1 - z) \cos \theta \left(H - \frac{M_S}{\chi_t} \sin \theta \right) = 0 \quad (51)$$

The choice of the free energy expression confirms that the pure magnetic behaviour is considered as reversible (e.g. without hysteresis).

Finally, let us examine the thermodynamical force associated with the z fraction of martensite:

$$\begin{aligned} \pi^{f*} = -\frac{\partial \rho G}{\partial z} = & \sigma \gamma - K_{12}(1 - 2z) \\ & + \mu_o M_S \left[(2\alpha - 1)H - \frac{M_S}{2\chi_a} (2\alpha - 1)^2 \right. \\ & \left. - H \sin \theta + \frac{M_S}{2\chi_t} \sin^2 \theta \right] \end{aligned} \quad (52)$$

This can be reduced to:

$$\begin{aligned} \pi^{f*} = & \sigma \gamma - K_{12}(1 - 2z) \\ & - \mu_o M_S^2 \left(\frac{(1 - 2\alpha) \sin \theta}{\chi_t} + \frac{(2\alpha - 1)^2}{2\chi_a} + \frac{\sin^2 \theta}{2\chi_t} \right) \end{aligned} \quad (53)$$

The mechanical behaviour of the considered material is highly irreversible e.g. with strong hysteresis. Hence the inequality of Clausius-Duhem can be written as:

$$dD = -\rho dG(\sigma, H, T, z) - \mu_o M dH - \varepsilon d\sigma \geq 0 \quad (54)$$

This expression can be reduced to:

$$dD = \pi^{f*} dz \geq 0 \quad (55)$$

Kinetic Equations and Minor Loops

To obtain the full characterization of the thermodynamic behaviour, the previous set of equations has to be completed with kinetic equations. The complete forward and reverse transformations (major loop) can so be obtained.

Let us note the equation (53) as:

$$\pi^{f*} = \Pi(\sigma, \alpha, \theta) - K_{12}(1 - 2z) \quad (56)$$

with:

$$\begin{aligned} \Pi(\sigma, \alpha, \theta) = & \sigma \gamma - \mu_o M_S^2 \left(\frac{(1 - 2\alpha) \sin \theta}{\chi_t} \right. \\ & \left. + \frac{(2\alpha - 1)^2}{2\chi_a} + \frac{\sin^2 \theta}{2\chi_t} \right) \end{aligned} \quad (57)$$

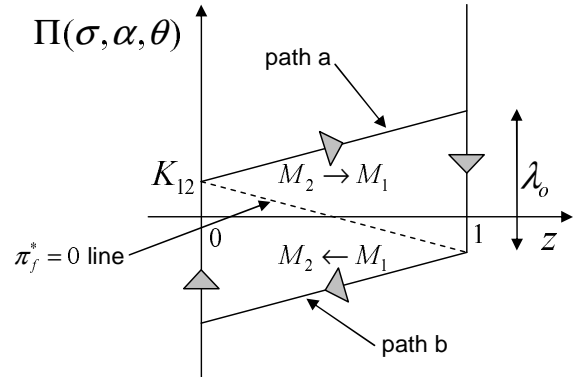


Figure 6. Thermodynamical force $\Pi(\sigma, \alpha, \theta)$ as a function of the M_1 martensite fraction $z \in [0, 1]$.

A major loop, i.e. a complete rearrangement from $z = 0$ to $z = 1$ (path a) and from $z = 1$ to $z = 0$ (path b), is reported on figure 6. Rearrangement begins when $\pi^{f*} \geq 0$ for the path a and when $\pi^{f*} \leq 0$ for the path b. After the rearrangement starts, the behaviour is modeled according to the following kinetic equation:

$$\dot{\pi}^{f*} = \lambda \dot{z} \quad (58)$$

This corresponds to a linear behaviour segment by segment represented on figure 6 for a major loop.

Unfortunately, the λ parameter can not be considered as a constant because it is related to the previous deformation history. To take this into account, the concept of memorized particular points is used in our model.

L. Org as et al. (2004) describe this concept: a special loop cycling is depicted in figure 7 with this behaviour. This loop cycling starts at $z = 1$ (point 1) and continues following the numerical order of the return points marked on the figure. The points (3,5,6,7,8) are considered from memorized points and the evolution of the material converges to these points.

During a complex cycling, all the starting points of the incomplete minor loops are memorized. Once a minor loop is closed, its starting point is forgotten and the material behaviour is identical to what it would have been if the minor loop had not been performed. The term of erasable micromemory has been introduced to characterize this behaviour: the parent loop is not affected by all the minor loop performed inside it.

Therefore the λ value can be considered as a function of these particular memorized points.

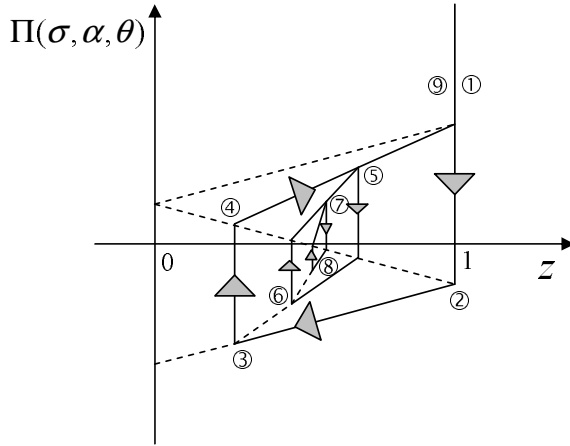


Figure 7. Description of a special loop cycling including the concept of memorized particular points.

Heat Equation

Furthermore, the heat equation can be expressed from the Gibbs free energy expression. The energy conservation principle induces the following equation:

$$\rho \dot{u}(\varepsilon, \vec{M}, s, z, \alpha, \theta) = -p_i + r_{ext} - \text{div} \vec{q} \quad (59)$$

where $p_i = -\underline{\Sigma} : \dot{\underline{\varepsilon}} - \mu_0 \vec{H} \cdot \dot{\vec{M}}$ is the power of internal effort, r_{ext} is the external heat contribution and \vec{q} is the heat flux density vector.

According to the Legendre transformation:

$$G(\underline{\Sigma}, \vec{H}, T, z, \alpha, \theta) = u(\underline{\varepsilon}, \vec{M}, s, z, \alpha, \theta) - Ts - \frac{\underline{\sigma} : \underline{\varepsilon}}{\rho} - \frac{\mu_0 \vec{H} \cdot \vec{M}}{\rho} \quad (60)$$

We can obtain:

$$\begin{aligned} \rho \dot{G} &= r_{ext} - \text{div} \vec{q} - \rho T \dot{s} - \rho s \dot{T} \\ &\quad - \dot{\underline{\sigma}} : \underline{\varepsilon} - \mu_0 \dot{\vec{H}} \cdot \vec{M} \end{aligned} \quad (61)$$

On the other hand:

$$\begin{aligned} \rho \dot{G} &= \frac{\partial \rho G}{\partial \sigma} \dot{\sigma} + \frac{\partial \rho G}{\partial H} \dot{H} + \frac{\partial \rho G}{\partial T} \dot{T} + \frac{\partial \rho G}{\partial z} \dot{z} \\ &\quad + \frac{\partial \rho G}{\partial \alpha} \dot{\alpha} + \frac{\partial \rho G}{\partial \theta} \dot{\theta} \\ &= -\varepsilon \dot{\sigma} - \mu_0 M \dot{H} - \rho s \dot{T} - \pi^{f*} \dot{z} + 0 \cdot \dot{\alpha} + 0 \cdot \dot{\theta} \end{aligned} \quad (62)$$

The combination of equations (61) and (62) gives:

$$\pi^{f*} \dot{z} = -r_{ext} + \text{div} \vec{q} + \rho T \dot{s} \quad (63)$$

By introducing the C_p parameter, the heat equation expression is finally written:

$$\pi^{f*} \dot{z} = -r_{ext} + \text{div} \vec{q} + \rho C_p \dot{T} \quad (64)$$

COMPARAISON BETWEEN MODEL PREDICTION AND EXPERIMENTS

Experimental Set-up

The MSM sample which is used comes from Adap-tamat Ltd. Its dimensions are $3 \times 5 \times 20$ mm. The martensite start temperature of the material is 36°C . Experiments are achieved at room temperature. A magnetic field is created by a coil and concentrated by a ferromagnetic circuit into an horizontal air-gap. Mechanical loading can be applied vertically (perpendicular to the magnetic field) with masses and a lever arm. A F.W. Bell 7010 teslameter enables to measure the magnetic field into the air-gap and a LAS 2010V laser sensor displays a vertical displacement information.

Equivalence Between Magnetic Field H and Stress Action σ : Yield Line (H, σ) for Martensite Variants Rearrangement Initiation

In a classical way, the rearrangement process starts when the thermodynamical force π^{f*} reaches a critical value called π_{cr} . For a constant temperature $T < A_s^0$:

$$\pi^{f*}(\sigma, H, z = 0) = \pi_{cr} \quad (65)$$

$$\begin{aligned} \Rightarrow \pi_{cr} &= \sigma \gamma - K_{12} \\ &\quad - \mu_0 M_S^2 \left(\frac{(1 - 2\alpha) \sin \theta}{\chi_t} + \frac{(2\alpha - 1)^2}{2\chi_a} + \frac{\sin^2 \theta}{2\chi_t} \right) \end{aligned} \quad (66)$$

Three situations must be examined.

- Zone I: no saturation appears in α and θ .

By using the following relations between α and H on one part and between θ and H on an another part:

$$2\alpha - 1 = \frac{\chi_a H}{M_S} \quad (67)$$

$$\sin \theta = \frac{\chi_t H}{M_S} \quad (68)$$

Finally, the critical thermodynamical force is:

$$\pi_{cr} = \sigma \gamma - K_{12} - \frac{\mu_0 H^2}{2} (\chi_t - \chi_a) \quad (69)$$

σ is affine in the square of H .

- Zone II: saturation appears in α but not in θ .

$$\alpha = 1, \sin \theta = \frac{\chi_t H}{M_S}$$

$$\pi_{cr} = \sigma \gamma - K_{12} - \frac{\mu_0 M_S^2}{2 \chi_a} + \mu_0 M_S H - \frac{\mu_0 \chi_t}{2} H^2 \quad (70)$$

σ is affine in a second degree polynomial in H .

- Zone III: saturation appears in α and θ .

$$\alpha = 1 \text{ and } \sin \theta = 1$$

$$\pi_{cr} = \sigma \gamma - K_{12} - \frac{\mu_0 M_S^2}{2} \left(\frac{1}{\chi_a} - \frac{1}{\chi_t} \right) \quad (71)$$

In this third situation σ reaches a constant value whatever H .

Figure 8 enables to compare experimental measurements to predictions with:

$$\mu_0 M_S = 0.65 \text{ T}, \chi_t = 0.82, \chi_a = 4, \pi_{cr} + K_{12} = 20.10^3 \text{ Pa}, \gamma = 0.055$$

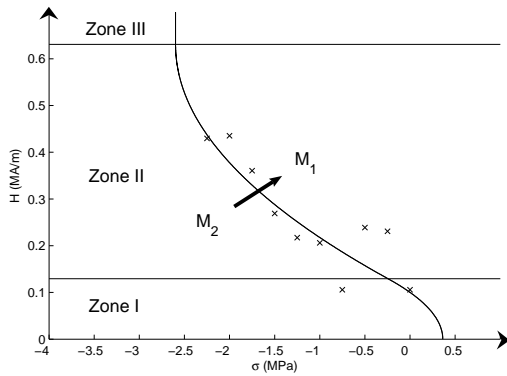


Figure 8. Yield line (H, σ) for martensite variants rearrangement initiation - model prediction (line) and experiments (points).

Mechanical Testing With or Without Magnetic Field

For these experiments, according to the hypothesis of the model, $z = 0$ and $\varepsilon = 0$ correspond to a sample composed of only M_2 variant (first situation). $z = 1$ and $\varepsilon = \gamma$ correspond to a sample composed of only M_1 variant (second situation). The starting point of these experiments corresponds to the second situation ($z = 1$). A compressive stress is applied to transform the M_1 variant into the M_2 variant then released ($\sigma = 0 \rightarrow \sigma = -|\sigma_{max}| \rightarrow \sigma = 0$).

The first experiment is conducted without magnetic field and the second one is conducted when a constant magnetic field is applied ($H = 600 \text{ kA/m}$). The parameters for the model are the same than before

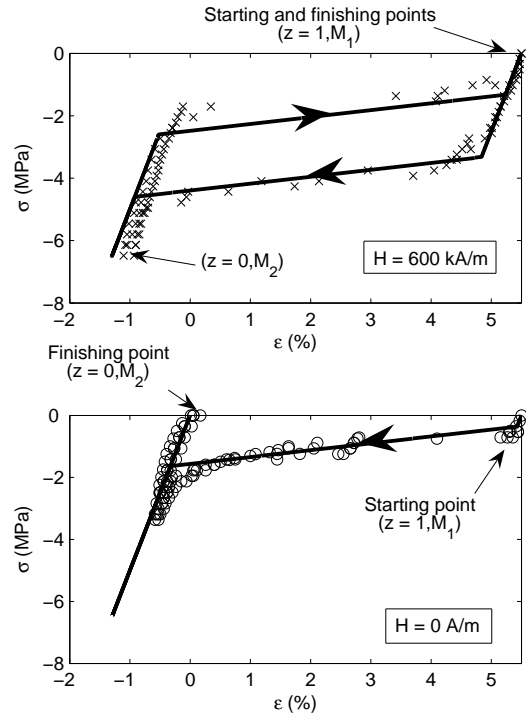


Figure 9. Strain vs stress plots for two different magnetic fields: model prediction (solid line) and experiments (crosses or circles).

with moreover: $\pi_{cr} = 0$, $\lambda_0 = 110.10^3 \text{ Pa}$ and $E = 500.10^6 \text{ Pa}$. The results are reported on the figure 9.

The first experiment enables to note that the finishing point does not correspond to the starting point whereas these two points correspond when the magnetic field is applied. The antagonistic effect between compressive stress and magnetic field is clearly demonstrated: the forward deformation is obtained by the stress when the backward deformation is recovered by the magnetic field. Moreover the predictions correspond well to the measurements.

Tests Under Constant Compressive Load

The starting point of this experiment corresponds to the first situation described above ($z = 0, \varepsilon = 0$). Then, a mass is applied to exert a constant compressive load σ ($z = 0, \varepsilon = \varepsilon^e$). By means of an electromagnet, a magnetic field is applied: two identical cycles ($H = 0 \rightarrow H = H_{max} \rightarrow H = 0$) are repeated. This enables to show first an external loop and secondly an internal loop.

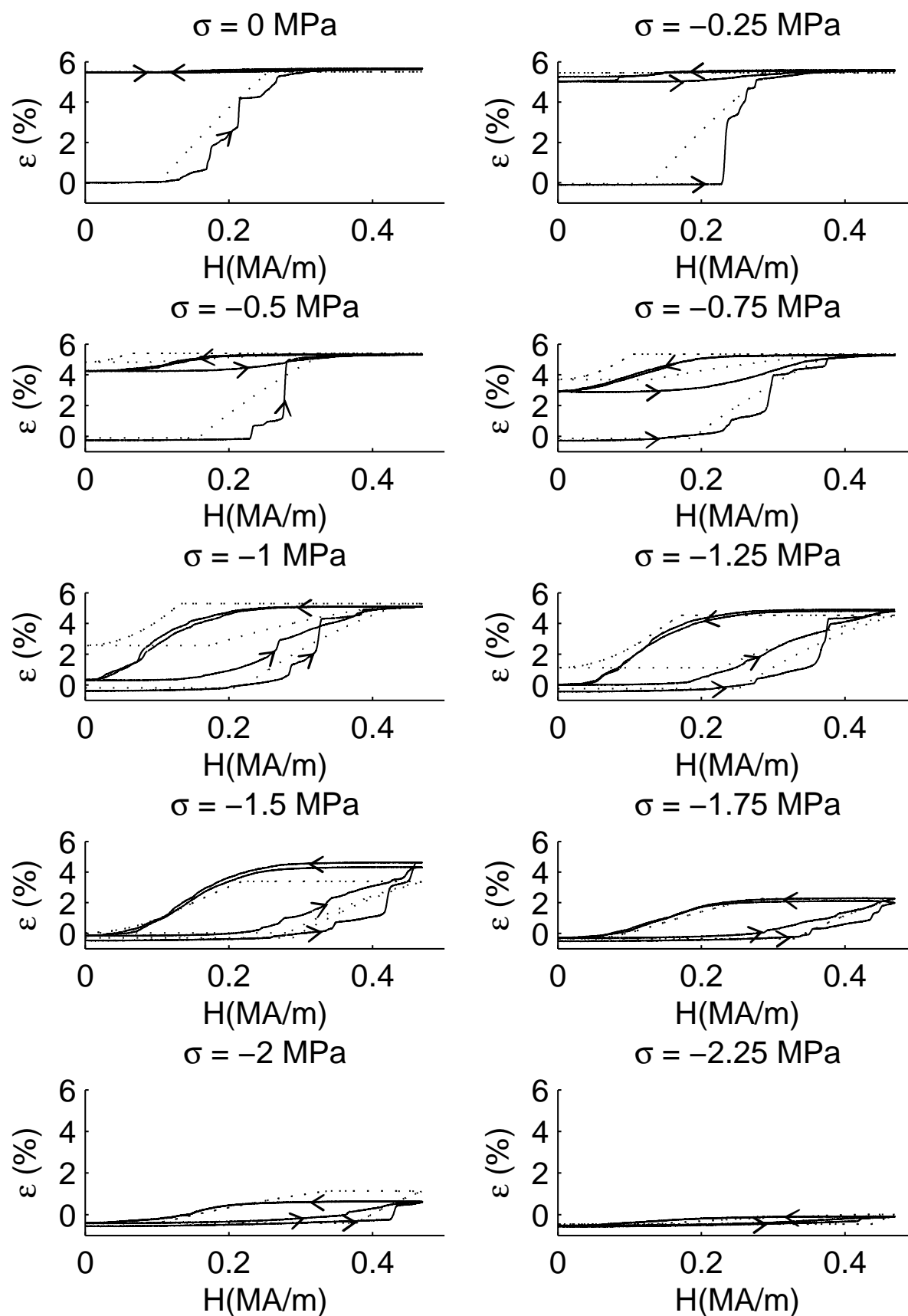


Figure 10. Strain vs magnetic field plots for different stresses: model prediction (dotted line) and experiments (solid line).

This experiment is conducted for different masses ($\sigma = 0, -0.25, -0.5, -0.75, -1, -1.25, -1.5, -1.75, -2$ and -2.25 MPa) and its results are reported on the figure 10.

We can notice some discrepancy between prediction and measurements, but, the model predicts relatively well the external and the internal loop. For this large pre-stress bandwidth, the results of the model are quite encouraging.

CONCLUSION

A new model integrating uniaxial stress action perpendicular to the magnetic field on a MSM Ni₂MnGa single crystal is built. The material behaviour is considered as magnetically reversible and mechanically irreversible. Thanks to the thermodynamical force associated to the martensite reorientation initiation process, an equivalence between magnetic field H and stress action σ is obtained. The curves describing the strain evolution ε as a function of magnetic field H , under constant external compression, are fairly fitted by the present model. Future works will concern the design and control of actuators using MSMs as active elements in a smart structure.

NOMENCLATURE

| | |
|---------------------------|--|
| M_i | = martensite variant i |
| G | = Gibbs free energy |
| G_{chem} | = chemical Gibbs free energy |
| G_{mech} | = mechanical Gibbs free energy |
| G_{mag} | = magnetic Gibbs free energy |
| G_{therm} | = thermal Gibbs free energy |
| $\underline{\Sigma}$ | = applied stress tensor |
| T | = temperature |
| \vec{H} | = magnetic field |
| z_o | = austenite volume fraction |
| $1 - z_o$ | = martensite volume fraction |
| z_k | = volume fraction of martensite variant k |
| n | = number of different variants |
| α | = proportion of the Weiss domain inside a variant |
| θ | = rotation angle of the magnetization vector |
| \vec{M} | = magnetization vector |
| u_o^A | = specific internal energy of the austenite phase |
| u_o^M | = specific internal energy of the martensite phase |
| s_o^A | = specific entropy of the austenite phase |
| s_o^M | = specific entropy of the martensite phase |
| T_o | = reference temperature |
| C_p | = specific heat |
| E_k^{tr} | = rearrangement deformation tensor |
| \underline{S} | = elastic compliance tensor |
| \bar{A} | = interaction parameter between austenite and martensite |
| K_{kl} | = interaction parameter between M_k and M_l |
| a_o | = lattice parameter of austenite phase |
| U_i | = phase transformation matrix from austenite into M_i |
| a | = long lattice parameter of martensite phase |
| c | = short lattice parameter of martensite phase |
| $\beta_a = \frac{a}{a_o}$ | |
| $\beta_c = \frac{c}{a_o}$ | |

| | |
|---------------------|--|
| Q | = rotation matrix |
| \vec{n} | = unit normal to the interface |
| \vec{a} | = "shear vector" |
| s' | = twinning shear |
| $z = z_1$ | for the simple case (M_1 fraction) |
| $1 - z = z_2$ | for the simple case (M_2 fraction) |
| σ | = applied stress for the simple case |
| M | = magnetization for the simple case |
| H | = magnetic field for the simple case |
| ε | = total strain for the simple case |
| ε^e | = elastic strain for the simple case |
| ε^{dtw} | = "detwinning" strain for the simple case |
| \underline{F}_i | = transformation gradient tensor of austenite into M_i |
| E | = Young's modulus |
| γ | = total uniaxial rearrangement strain |
| ρ | = mass density |
| u_{mag} | = magnetic energy |
| \vec{B} | = magnetic flux density |
| u_{mag}^* | = magnetic co-energy |
| μ_o | = permeability of the vacuum |
| M_S | = saturation magnetization |
| χ_t | = magnetic susceptibility for hard magnetization direction |
| χ_a | = magnetic susceptibility for easy magnetization direction |
| A_o^s | = austenite start temperature at stress free state |
| π^{f*} | = thermodynamical force associated with z |
| dD | = dissipation increment |
| λ | = kinetic parameter |
| λ_o | = kinetic parameter for major loop |
| u | = specific internal energy |
| p_i | = power of internal effort |
| r_{ext} | = external heat source |
| \vec{q} | = heat flux density vector |
| s | = specific entropy |
| π_{cr} | = critical value for thermodynamical force π^{f*} |

REFERENCES

- Ball, J. and James, R. 1987. "Fine phase mixtures as minimizers of energy". *Arch. Rational. Mech. Anal.*, 100:13–52.
- Ball, J. and James, R. 1992. "Proposed experimental tests of the theory of fine microstructure and the two well problem". *Phil. Trans. Royal Soc. London, A* 338:389–450.
- Bhattacharya, K. 2003. *Microstructure of Martensite : Why It Forms and How It Gives Rise to the Shape-Memory Effect*. Oxford series on materials modelling.
- Buisson, M., Patoor, E., and Berveiller, M. 1991. "Comportement global associé aux mouvements d'interfaces entre variantes de martensite". *C.R. Acad. Sci. Paris*, 313(2):587–590.
- Creton, N. 2004. *Etude du comportement magnéto-mécanique des alliages à mémoire de forme de type Heusler Ni-Mn-Ga*. PhD thesis, Université de Franche-Comté (France).
- Hane, K. F. 1999. "Bulk and thin film microstructures in untwinned martensites". *Journal of the Mechanics and Physics of Solids*, 47(9):1917–1939.
- Henry, C., Bono, D., Feuchtwanger, J., Allen, S., and O'Handley, R. 2002. "Field-induced actuation of single crystal ni-mn-ga". *J. of Applied Phys.*, 91:7810–7811.
- Hirsinger, L., Creton, N., and Lexcellent, C. 2004. "From crystallographic properties to macroscopic detwinning strain and magnetisation of ni-mn-ga magnetic shape memory alloys". *J. Phys. IV*, 115:111–120.

- Hirsinger, L. and Lexcellent, C. 2002. "Modelling detwinning of martensite platelets under magnetic and (or) stress actions in ni-mn-ga alloys". *J. of Magnetism and Magnetic Materials*, 254-255:275-277.
- James, R. and Zhang, Z. 2005. "A way to search for multiferroic materials with "unlikely" combinations of physical properties". *to appear in "Interplay of Magnetism and Structure in Functional Materials"* (ed. L. Manosa, A. Planes, A.B. Saxena), Springer Verlag.
- Landau, L., Lifshitz, E., and Pitaevskii, L. 1984. *Electrodynamics of Continuous Media : Volume 8 (Course of Theoretical Physics) (2nd Edition)*. Butterworth-Heinemann.
- Lexcellent, C., Goo, B., Sun, Q., and Bernardini, J. 1996. "Characterization, thermodynamical behaviour and micromechanical-based constitutive model of shape memory cu-zn-al single crystals". *Acta Met.*, 44(9):3773-3780.
- Likhachev, A., Sozinov, A., and Ullakko, K. 2004. "Different modeling concepts of magnetic shape memory and their comparison with some experimental results obtained in ni-mn-ga". *Materials Science and Engineering A*, 378:513-518.
- Marioni, M., O'Handley, R., and Allen, S. 2003. "Pulsed magnetic field-induced actuation of ni-mn-ga single crystals". *Applied Physics Letters*, 83:3966-3968.
- Mori, T. and Tanaka, K. 1973. "Average stress in matrix and average elastic energy of materials with misfitting inclusions". *Acta Met.*, 21:571-574.
- Mullner, P., Chernenko, V., and Kostorz, G. 2003. "Stress-induced twin rearrangement resulting in change of magnetization in a ni-mn-ga ferromagnetic martensite". *Scripta Mat.*, 49:129-133.
- Orgéas, L., Vivet, A., Favier, D., Lexcellent, C., and Liu, Y. 2004. "Hysteretic behaviour of a cu-zn-al single crystal during superelastic shear deformation". *Scripta Materialia*, 51:297-302.
- Patoo, E., Eberhardt, A., and Berveiller, M. 1998. "Thermomechanical modelling of shape memory alloys". *Arch. Mech.*, 40-5,6:775-794.
- Roubíček, T. 2004. "Models of microstructure evolution in shape memory alloys". In *Nonlinear Homogenization and its Applications to Composites, Polycrystals and Smart Materials*, pages 269-304. P. Ponte Castaneda et al. eds., Kluwer.
- Sommerfeld, A. 1964. *Thermodynamics and Statistical Mechanics*. Academic Press.
- Sun, Q. and Hwang, K. 1993. "Micromechanics modelling for the constitutive behavior of polycrystalline shape memory alloys - i : Derivation of general relations". *J. Mech. Phys. Solids*, 41(1):1-17.
- Suorsa, I., Tellinen, J., Aaltio, I., Pagounis, E., and Ullakko, K. 2004. "Design of active element for msm-actuator". In *ACTUATOR 2004 / 9th International Conference on New Actuators*, Bremen (Germany).